Anal. Chem. **2000,** *72,* 2035−2041

An Electrochemical Impedance Measurement Technique Employing Fourier Transform

Jung-Suk Yoo and Su-Moon Park*

Department of Chemistry, Pohang University of Science and Technology, Pohang 790-784, Korea

We describe a novel technique for measuring electrochemical impedance, in which the electrode potential is ramped to a desired bias potential and a small potential step is applied to the working electrode after a short time delay. Fourier transform of the first derivative of the current signal thus obtained provides ac currents in the frequency domain, which allows the computation of impedances of the electrode/electrolyte interface in the whole frequency range. A home-built data acquisition system for these measurements and the results obtained therefrom were used for the measurements. The advantage of the technique includes an extremely short time of less than 1 ms for impedance measurements in the whole frequency region while equilibrium conditions of the electrochemical system are being maintained before and after the measurements, among many others. This technique is expected to revolutionize electrochemical measurements and to find important applications such as in situ measurements during battery cycling, corrosion testing, and other electrochemical experiments.

The efficiency of an electron-transfer reaction in an electrochemical system is determined by the impedance of the electrode/electrolyte interface, which in turn is determined by the electrode material and other experimental parameters.[1] Impedance measurements of such a system allow a complete description of the electrode/electrolyte interface with an equivalent circuit for a given electron-transfer reaction under given experimental conditions.[2] For this reason, impedance measurements are frequently used for studying the state of electrodes in energy conversion devices including secondary batteries and fuel cells as well as in corrosion.[3]

A few techniques are available for impedance measurements including methods using frequency response analyzers (FRAs) or lock-in amplifiers.[4] Most of these methods employ analysis of the response signal (current) after applying a small ac voltage at a given frequency, which is overlayed on a bias potential. Thus, the small ac voltage of the given frequency is generated by a machine and applied to the working electrode. The impedance is then measured at each frequency. This needs to be repeated for a whole range of frequencies of interest. In the FRA method, e.g., the current signal obtained after the application of the ac voltage to the electrochemical cell is multiplied by a reference sine, or cosine, signal to resolve imaginary and real parts of the impedance.[5] The current signal thus obtained is integrated over a few periods of the sine wave to reduce noise. Because of the frequency sweep and the signal integration, it takes a long time to make impedance measurements in a full frequency region, at times more than a few hours, particularly when the frequencies of as low as milli- or submillihertz are included. When the electrochemical system is unstable, the problem of maintaining equilibrium conditions is even more serious than the time taken for measurements, which is often the case during electrochemical reactions. Also, most software programs written for impedance measurements wait, by monitoring dc currents, until the electrochemical system becomes stabilized before the impedance measurements are made,[6] which takes additional time for measurements.

Efforts made to implement Fourier transform into the impedance measurement systems to alleviate these problems in the past did not greatly improve the shortcomings described above. Pilla[7] reported what he called a “transient impedance technique”, in which the time domain electrode response of an arbitrary perturbation was converted to the frequency domain data using La Place transform. Later, a similar approach was described by Smyrl.[8] Smith and co-workers[9] took advantage of Fourier transform for impedance measurements also. A few more similar studies have been reported since then.[10] The method uses a mixed signal of ac waves of about 20 different frequencies as an excitation

* Corresponding author: (e-mail) smpark@postech.edu.

(1) See, for example: (a) Bard, A. J.; Faulkner, L. R. *Electrochemical Methods*; John Wiley & Sons: New York, 1980. (b) Bockris, J. O'M.; Khan, S. U. M. *Surface Electrochemistry*; Plenum Press: New York, 1993 among many others.

(2) Macdonald, J. R. *Impedance Spectroscopy*; Wiley/Interscience: New York, 1987 among many others.

(3) See, for example: Linden, D., Ed. *Handbook of Batteries*; 2nd ed.; McGraw-Hill: New York, 1995. For applications to corrosion research, see Chapter 4 of ref 2.

(4) See Chapter 3 of ref 2.

(5) Gabrielli, C. *Identification of Electrochemical Processes by Frequency Response Analaysis*; Technical Report No. 004/83; Solartron: Farnborough, Hamphshire, England, 1984.

(6) See, for example: *1255 H. F. Frequency Response Analyzer Operating Manual*; Solartron: Farnborough, Hamphshire, England, 1994.

(7) Pilla, A. *J. Electrochem. Soc.* **1970**, *117*, 467.

(8) Smyrl, W. *J. Electrochem. Soc.* **1985**, *132*, 1551.

(9) (a) Creason S. C.; Smith, D. E. *J. Electroanal. Chem.* **1972**, *36*, 1. (b) *J. Electroanal. Chem.* **1972**, *40*, 1. (c) Creason, S. C.; Hayes, J. W.; Smith, D. E. *Anal. Chem.* **1973,** *47*, 9. (d) Creason S. C.; Smith, D. E. *Anal. Chem.* **1973**, *47*, 2401. (e) Smith, D. E. *Anal. Chem.* **1976**, *48*, 221A. (f) Smith, D. E. *Anal. Chem.* **1976**, *48*, 517A. (g) Schwall, R. J.; Bond, A. M.; Loyd, R. J.; Larsen, J. G.; Smith, D. E. *Anal. Chem.* **1977**, *49*, 1797. (h) Schwall, R. J.; Bond, A. M.; Smith, D. E. *Anal. Chem.* **1977**, *49*, 1805. (i) Schwall, R. J.; Bond, A. M.; Smith, D. E. *J. Electroanal. Chem.* **1977**, *85*, 217. (j) Bond, A. M.; Schwall, R. J.; Smith, D. E. *J. Electroanal. Chem.* **1977**, *85*, 231. (k) O'Halloran, R. J.; Schaar, J. E.; Smith, D. E. *Anal. Chem.* **1978**, *50*, 1073. (l) Crzeszczuk M.; Smith, D. E. *J. Electroanal. Chem.* **1983**, *157*, 205.

10.1021/ac9907540 CCC: $19.00
Published on Web 03/24/2000

source, and the resultant response current is Fourier transformed to obtain ac currents in the frequency domain. This method, while it appears to offer advantages the same as or similar to the one to be described in this work, suffers from a disadvantage that as long a time as needed to make measurements in the lowest frequency used in the mixed excitation signal *must* be spent to obtain information in the frequency region. This is because the sampling theorem requires the time for data acquisition at a minimum frequency. Thus, the method does not in effect offer much advantage over the FRA method itself, except that the time required for running experiments at each frequency would be saved, as only one such time is necessary when the mixed-signal Fourier transform (FT) method is used.

In our present paper, we describe preliminary results obtained for a novel impedance measurement technique employing Fourier transform. In this technique, the data acquisition time required by the sampling theorem is overcome by taking the first derivative of a small chronoamperometric signal, which is then Fourier transformed into ac signals and impedance is computed therefrom.

THEORETICAL CONSIDERATIONS

Since an ideal Dirac δ function contains components of *all* frequencies with an identical magnitude and an identical phase,[11] one may apply a voltage signal having the shape of the Dirac δ function in the time domain and the resulting current signal is then converted into the frequency domain. The impdance can then be computed from the resulting ac current in the frequency domain. While this approach appears simple for the measurement of the impedance, it is very difficult, if not impossible, to actually implement the method to an electrochemical system. This is because the Dirac δ (impulse) function has almost no base with a height of an infinitely large magnitude. It is not only very difficult to construct such a voltage signal by hardware but also dangerous to apply it to an electrochemical cell as the electrochemical reaction system may be damaged by such a large voltage spike.

To circumvent this problem, we took advantage of a theorem[11] that a linear system, which responds to an excitation voltage signal $v(t)$ with a current signal $i(t)$, responds also with its derivative or integrated form of the signals, i.e., $i'(t)$ or $\int i(t)$, upon imposing derivative or integrated forms of the original excitation signals, i.e., $v'(t)$ or $\int v(t)\,dt$. The only problem with this theorem in our case is that the electrochemical system is *not* linear in a wide range of overpotential, as the current−voltage curve follows the Butler−Volmer equation, which has two exponential terms.[12] The nonlinearity problem may be, however, avoided or minimized when the excitation signal is small, as an exponential function (i.e., the resulting current in our case) behaves like a linear one when its independent variable component (i.e., excitation voltage in our case) is small. The Butler−Volmer equation is often linearized when the change in overpotential is small.[13] The system

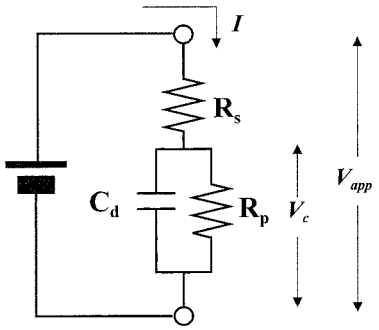

Figure 1. A typical equivalent circuit for an electrochemical cell. Here R_s is the solution resistance, R_p is the polarization resistance, and C_d is the double-layer capacitance.

thus linealized in a limited region is called a piecewise linear system.[14] Thus, this theorem and the linearity approximation described above would allow us to use a *small* potential step (10 mV) as an excitation signal, which is the integrated form of the Dirac δ function. When the first derivative is taken for the response current, it would be the same as the current response signal if the voltage signal of the Dirac δ function had been applied. Fourier transform of this derivative signal gives ac current signals in the frequency domain.

For a typical equivalent circuit shown in Figure 1, where R_s is the solution resistance, R_p is the polarization resistance during electron transfer, and C_d is the double-layer capacitance, the impedance for the electrode/electrolyte interface has a familiar expression,[15]

$$Z = R_s + \frac{R_p}{1 + jR_pC_d\omega} = R_s + \frac{R_p}{1 + R_p^2C_d^2\omega^2} + \frac{jR_p^2C_d}{1 + R_p^2C_d^2\omega^2} \quad (1)$$

where $\omega = 2\pi f$, with f being frequency. The second term on the right-hand side is a *real* term of the impedance while the third term is *imaginary*.

Now, let us see what happens when a potential step, $V{\cdot}U(t)$, where V is a magnitude of the voltage step and $U(t)$ is the unit step function, is applied. For an applied potential, V_{app}, we have the following relation from the Kirchoff rule:

$$V_{app} = V_c + \left(\frac{V_c}{R_p} + C_d\frac{dV_c}{dt}\right)R_s = V_c\left(1 + \frac{R_s}{R_p}\right) + R_sC_d\frac{dV_c}{dt} \quad (2)$$

where V_c is the potential drop across the RC network as indicated in Figure 1. This equation can be rearranged to give the following form upon replacing the V_{app} with the stepped potential, $V{\cdot}U(t)$:

(10) (a) Bond, A. M. *J. Electroanal. Chem.* **1974**, *50*, 285. (b) Ühlken, J.; Waser, R.; Wiese, H. *Ber. Bunsen-Ges. Phys. Chem.* **1988**, *92*, 730. (c) Házi, J.; Elton, D. M.; Czerwinski, W. A.; Schiewe, J.; Vincente-Beckett, V. A.; Bond, A. M. *J. Electroanal. Chem.* **1997**, *437*, 1.

(11) (a) Gabel, R. A.; Roberts, R. A. *Signals and Linear Systems*; Wiley: New York, 1987. (b) Carlson, A. B. *Communication Systems*; McGraw-Hill: Singapore, 1986. (c) Ifeachor, E. C.; Jervis, B. W. *Digital Signal Processing*; Addision-Wesley: New York, 1993.

(12) See Chapter 3 of refs 1a and b.

(13) See, for example: Bard, A. J.; Faulkner, L. R. *Electrochemical Methods*; John Wiley: New York, 1980; Chapter 3, p 105.

(14) Sedra, A. S.; Smith, K. C. *Microelectronic Circuits*; Saunders College Publications: Tokyo, Japan, 1991.

(15) See, for example: Gabrielli, C. *Identification of Electrochemical Processes by Frequency Response Analysis*; Technical Report No. 004/83; Schlumberger Tenologies, Hampshire, England, 1984.

$$\frac{dV_c}{dt} + \frac{R_p + R_s}{R_p R_s C_d} V_c = \frac{V_{app}}{R_s C_d} = \frac{V \cdot U(t)}{R_s C_d} \quad (3)$$

Upon integrating eq 3, we obtain

$$V_c = U(t) \frac{V \cdot R_p}{R_p + R_s} (1 - e^{-((R_p+R_s)/R_p R_s C_d)t}) \quad (4)$$

Now, the current flowing across the *RC* circuit can be written as

$$I = C_d \frac{dV_c}{dt} + \frac{V_c}{R_p}$$
$$= U(t)\left[\frac{V}{R_s} e^{-((R_p+R_s)/R_p R_s C_d)t} + \frac{V}{R_s + R_p}(1 - {}^{-((R_p+R_s)/R_p R_s C_d)t})\right] \quad (5)$$

Hence the current obtained from the potential step is

$$I_s(t) = U(t)\left[\frac{V}{R_s} e^{-((R_p+R_s)/R_p R_s C_d)t} + \frac{V}{R_s + R_p}(1 - e^{-((R_p+R_s)/R_p R_s C_d)t})\right] \quad (6)$$

The current for an impulse function in the time domain is obtained by taking a first derivative of eq 6, i.e.,

$$I_p(t) = \frac{dI_s(t)}{dt} = \delta(t)\frac{V}{R_s} - U(t)\frac{V}{R_s{}^2 C_d} e^{-((R_p+R_s)/R_p R_s C_d)t} \quad (7)$$

The current *in the frequency domain* is now obtained by Fourier transform of eq 7. We then have a current expression in the frequency domain,

$$I_F(\omega) = \int_{-\infty}^{\infty} I_p(t) e^{-j\omega t}\, dt$$
$$= \int_{-\epsilon}^{+\epsilon} \delta(t)\frac{V}{R_s} e^{-j\omega t}\, dt - \int_0^{\infty} U(t)\frac{V}{R_s{}^2 C_d} e^{-((R_p+R_s)/R_p R_s C_d)t}\, e^{-j\omega t}\, dt$$
$$= \frac{V}{R_s} - \frac{V}{R_s{}^2 C_d}\frac{1}{\left(\frac{R_p + R_s}{R_p R_s C_d} + jw\right)} \quad (8)$$

Since the impedance for the circuit shown in Figure 1 is obtained by simply dividing *V* by the current just obtained (eq 8), the impedance takes the form,

$$Z = \frac{V}{I_F(\omega)} = \frac{R_s(1 + (R_s/R_p) + R_s C_d j\omega)}{(R_s/R_p) + R_s C_d j\omega} =$$
$$R_s + \frac{R_s}{(R_s/R_p) + R_s C_d j\omega} = R_s + \frac{R_p}{1 + R_p C_d j\omega} \quad (1a)$$

which is identical to the impedance expression, eq 1, which we derived for an ac voltage applied across the equivalent circuit shown in Figure 1. Thus, we see that the impedance can also be obtained by applying a potential step, followed by taking Fourier transform of the first derivative signal of the current signal obtained.

This approach would limit the observable frequency range imposed by the sampling theorem, which requires that the highest observable frequency be half of the sampling frequency and the frequency resolution be the sampling frequency divided by the total number of observed points. If one wishes to observe down to the millihertz range, one *must* observe for thousands of seconds. Our approach circumvents this requirement, not violating it. To obtain a full frequency response in the frequency domain, we must use the discrete time Fourier transform (DTFT) algorithm, which has the form,

$$F(\omega) = \sum_{n=-\infty}^{\infty} f(n) e^{-j\omega n \Delta t} \quad (9)$$

where $f(n)$ is the nth observed signal and Δt is the sampling interval. This algorithm generates a continuous function of ω, because the observation is made in the time window between $-\infty$ and ∞. When, however, $f(n) = 0$ in the range of $-\infty < n < 0$ and $n_o < n < \infty$, where n_o is a finite number smaller than ∞, eq 9 reduces to

$$F(\omega) = \sum_{n=0}^{n_0} f(n) e^{-j\omega n \Delta t} \quad (10)$$

and then the transform generates a continuous function of ω by transforming between the two limits, $-\infty$ and ∞, as in eq 9, although only $n_o + 1$ points were sampled.[11,16] On the other hand, if we take only $n_o + 1$ samples *without* knowing the component of $f(n)$ outside the time window bounded by n_o and the resultant signal is Fourier transformed, the frequency resolution would be just the sampling frequency divided by $n_o + 1$. In other words, the observation time is infinitely large for the former case *provided we already know* that signals are 0 for the range between $t < 0$ and $t > n_o$, while it is just $(n_o + 1)\Delta t$ for the latter case.

In our case, *we already know* the first derivative of the chronoamperometric signal is zero before a voltage step is applied and decays to zero a short time after a voltage step is applied, as can be confirmed from the theoretical calculation using eq 7 and the experimental data shown in Figure 6 (see below). In other words, the impulse responses have observable nonzero data points within a limited time range, which is specified as n_o, decaying to 0 outside this range. Nonetheless, use of the discrete time Fourier transform performed between $-\infty$ and ∞ according to eq 9 allows the observation of signals to be extended down to almost the dc region.[16] Thus, in principle, our method would allow possible measurements of impedance data between the half of the highest sampling frequency (~50 kHz) down to almost dc.

EXPERIMENTAL SECTION

For these measurements to be meaningful, one should have a *very stable* and *fast rising* potentiostat, which is not readily available

(16) See, for example: Chapter 5 of ref 11a.

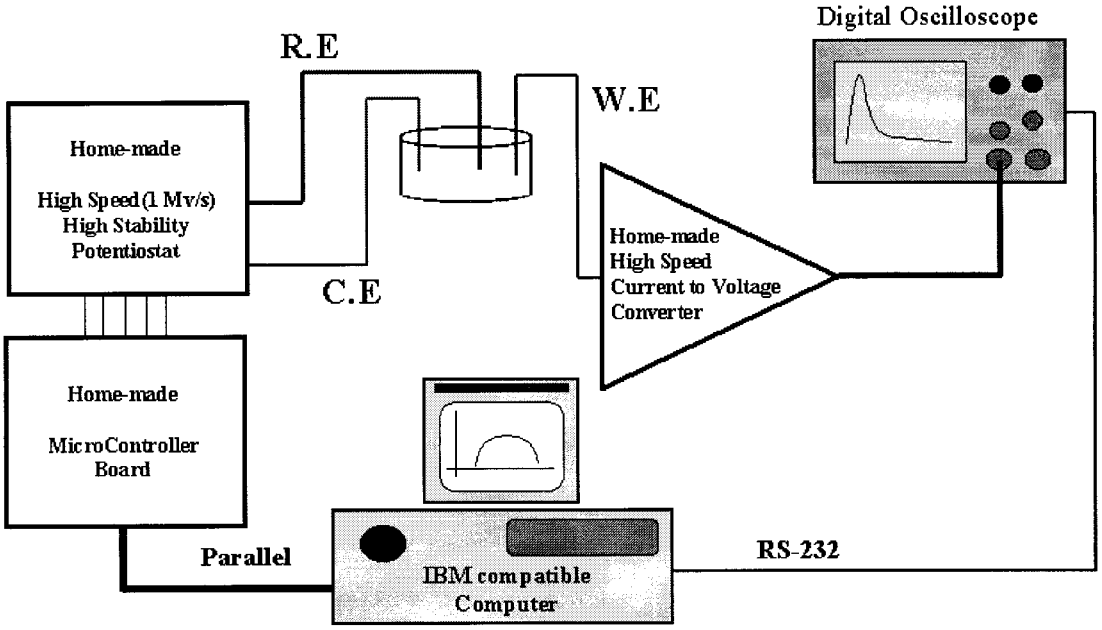

Figure 2. Schematic diagram of the impedance measurement system. The potentiostat has a slew rate of 1 MV/s with a very high stability. The voltage signal converted from the current signal was digitized using an HP model 54645D 100-MHz digital oscilloscope. The repetitive pulse signals followed by the ramps (see Figure 3) were outputted by a fast digital-to-analog converter on the microcontroller board for oscilloscope sampling.

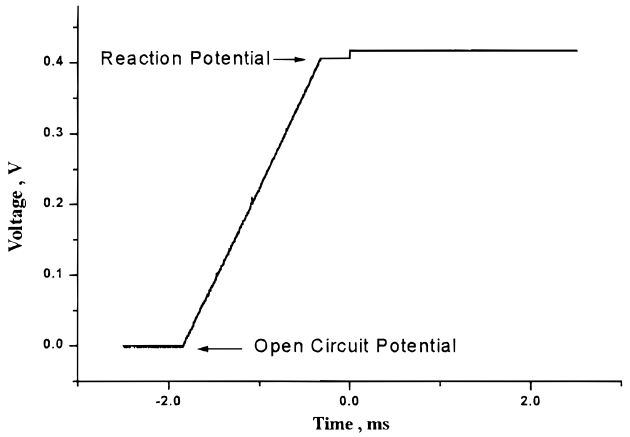

Figure 3. The ramp signal followed by a pulse signal applied to the working electrode. The potential is ramped from an open circuit potential to a desired base potential, 406 mV in this case, and a 10 mV pulse is applied after a 300-μs delay.

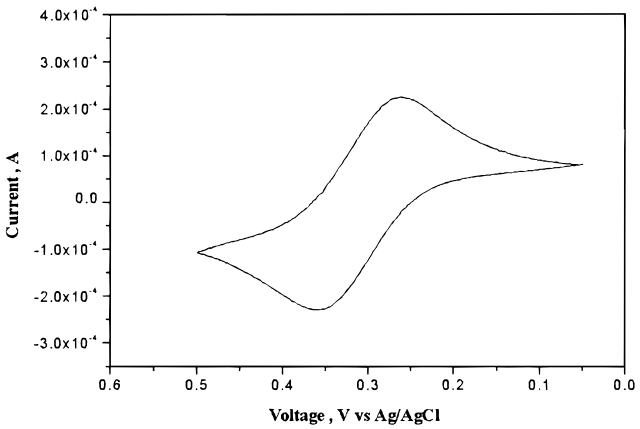

Figure 4. A typical cyclic voltammogram recorded at 50 mV/s for oxidation of 50 mM $Fe(CN)_4^{4-}$ in a 1 M KNO_3 solution at a platinum disk electrode of 2 mm in diameter.

on the market. We constructed such a potentiostat, which had a slew rate of 1 MV/s. Figure 2 shows a schematic diagram of the system configured in our laboratory. The digitization of the signal must be very fast as well because recording the signal rise during the measurement of the small chronoamperometric signal is very important not to lose any information contained in a relatively narrow time zone (see below). We used an 8-bit Hewlett-Packard model HP 54645D 100-MHz digital oscilloscope to digitize the signal. To make measurements at a given bias potential, the potential is ramped to a desired value to allow the concentration profile to be established and a small step (10 mV) is applied to the working electrode after a short time delay (see Figure 3). The dc current is then measured and its derivative is taken for the computation of impedance.

To test the newly developed technique, we used an electrochemical system containing 50 mM $K_4Fe(CN)_6$ and 1.0 M KNO_3 in water. The platinum disk (diameter 2 mm), platinum gauze, and Ag|AgCl (in saturated KCl) electrodes were used as working, counter, and reference electrodes, respectively.

RESULTS AND DISCUSSION

Figure 3 shows a typical excitation signal used for the electrochemical cell. The cell potential was ramped from an open circuit voltage of 0 V to 406 mV, and a 10 mV step was applied to the working electrode after a time delay of 0.3 ms. Figure 4 shows a typical cyclic voltammogram (CV) obtained at a scan rate of 50 mV/s. The CV shows that the electrochemical reaction is a reversible one-electron process under the given experimental conditions as can be seen from the peak separation of 60 mV.

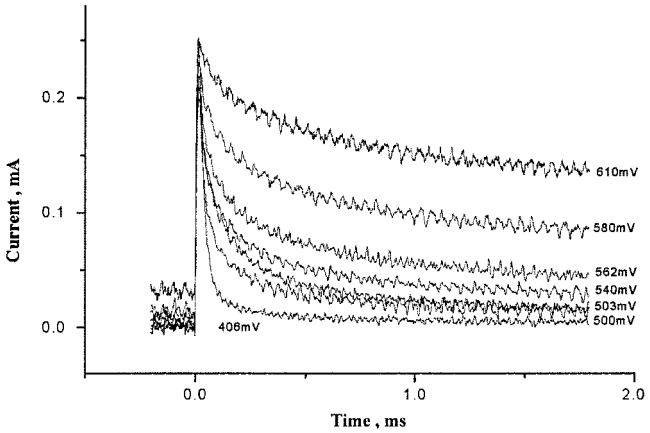

Figure 5. Transient currents observed at indicated base potentials after the pulses are applied.

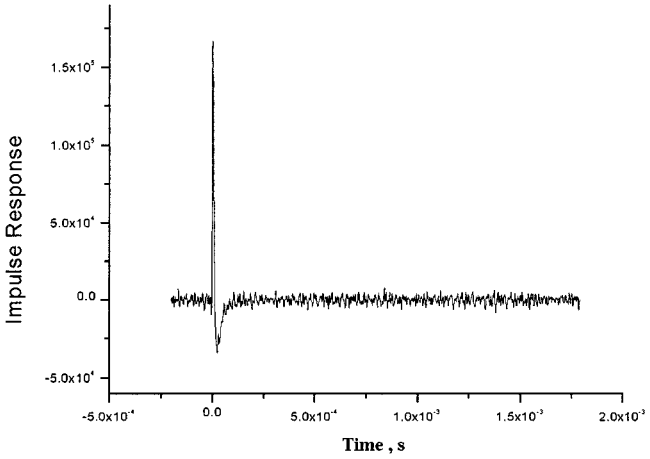

Figure 6. A typical derivative signal of the transient current, which was taken from the current signal recorded at the base potential of 406 mV shown in Figure 5.

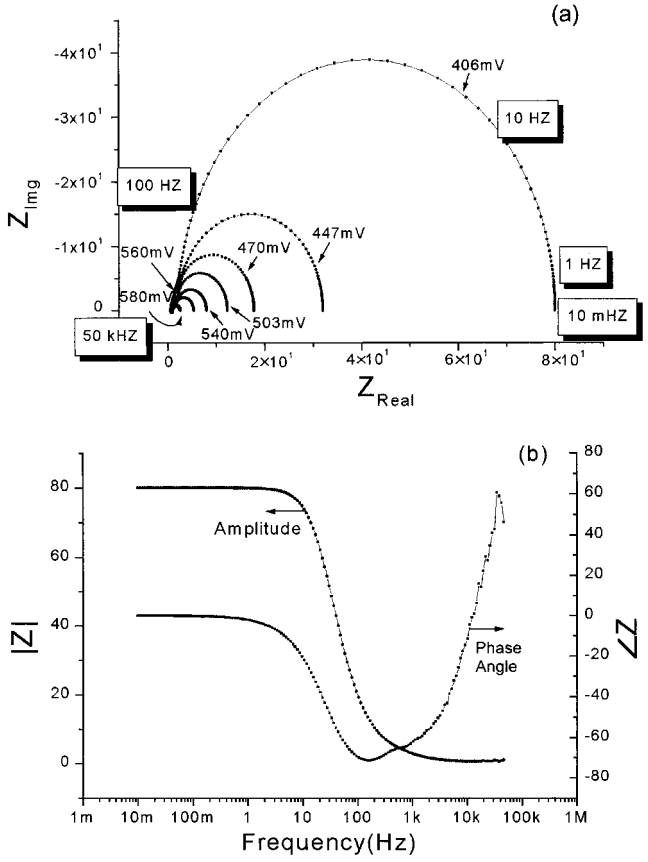

Figure 7. (a) Nyquist plots at various bias potentials obtained from the Fourier transform of the derivative signals at various bias potentials. While the calculation can be done in any frequency region, impedance values were computed between 50 kHz and 0.01 Hz (26 points/decade) at each potential for a shorter computational time. (b) Bode plots i.e., $|Z_{real}|$ vs log ω and phase angle vs log ω plots, for the data shown in (a).

Typical current responses obtained at various bias potentials after the subtraction of the background current are shown in Figure 5. Figure 6 shows a typical derivative signal of the current signal recorded at 406 mV. As can be seen from Figure 6, the current spike of as large as ~170 000 A/s is observed in the derivative signal, which would have been observed if an impulse voltage signal with the shape of the Dirac δ function had been applied. Figure 7a shows the impedance plots obtained at various bias potentials by transforming derivative signals such as that shown in Figure 6 according to the algorithm expressed as eq 9. Figure 7b shows Bode plots for the data obtained at 406 mV. While the amplitude vs log ω plot shows an ideal behavior, that of phase angle vs log ω shows somewhat an anomaly in that the phase angle approaches to ~90° in the high-frequency region. This suggests that the electrochemical cell represented by the $R-C$ network behaves more like an inductor at high frequencies. We believe this is because the wiring between the measurement and electrochemical systems may act like a coil and produces the inductance. It is clearly seen from the amplitude vs log ω plot that the R_p value is obtained from the data at low frequencies, while the R_s value is calculated from the high-frequency region. This plot (amplitude vs log ω) behaves as ideally as it can.

To compare the results with those obtained from the conventional method, results obtained using a Solartron model 1255 FRA are shown in Figure 8a and corresponding Bode plots for the data obtained at 406 mV are shown in Figure 8b. In Bode plots, it is difficult to obtain much information from either the amplitude vs log ω or phase angle vs log ω plots. Both are very ill defined. It is particularly interesting to note that the $R-C$ network behaves like a resistor at high frequencies. This is also attributed to the complex electronics of the 1255 FRA, which affects the impedance behavior of the whole system.

There are a few points to be noticed from our results. First, it is seen from Figures 5 and 6 that the measurements are made within a few milliseconds, typically less than 2 ms, when our FT method is used. This is because the Dirac δ function contains *all* the frequency components in a short time period. In fact, the most important measurements are made in a fraction of a millisecond as shown in Figure 6. Outside this range, we see that the impulse current signal is safely regarded as zero; however, the information in the low-frequency range is obtained by using the DTFT between $-\infty$ and ∞ as already pointed out. As mentioned, it takes hours to get the same amount of information for the conventional method.

Second, the Warburg impedances seen in Figure 8, when the conventional FRA method is used, are not seen in Figure 7 even

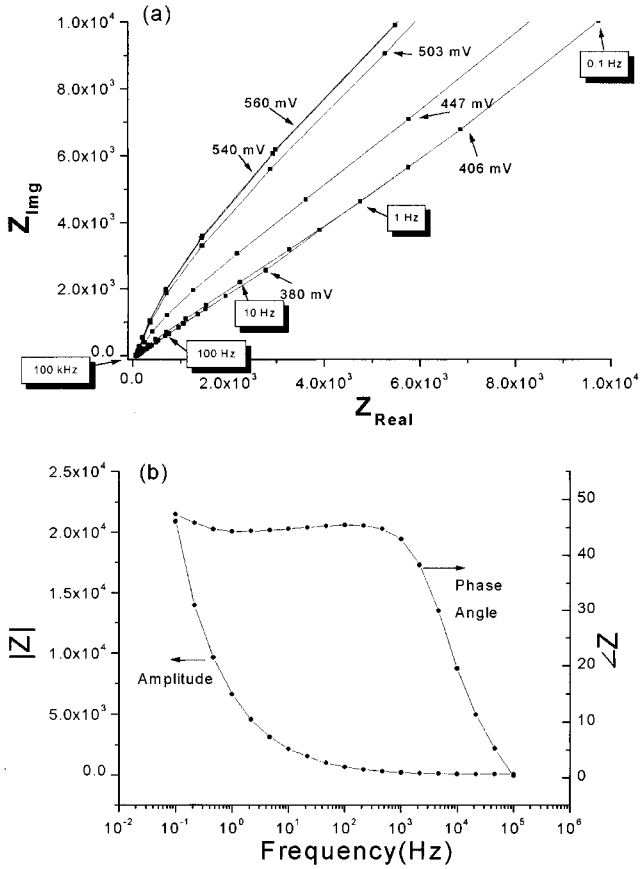

Figure 8. (a) Nyquist plots at various bias potentials recorded using the Solartron model 1255 FRA under the same experimental conditions as used for the data shown in Figure 7. Impedance values were measured between 50 kHz and 0.01 Hz (3 points/decade) to compare with results shown in Figure 7. (b) Bode plots, i.e., $|Z_{real}|$ vs log ω and phase angle vs log ω plots, for the data shown in (a).

at very low frequencies. We believe this is because the voltage excitation process is so short that the diffusion profile is not disturbed much within the experimental time frame and the mass transfer is not a limiting factor in determining the rate of electron transfer accross the electrode/electrolyte interface. As a result, the impedance measurements at much higher overpotentials for oxidation of the ferrocyanide ion were shown to be possible (Figures 4 and 7). Similar impedance plots were obtained at high rotation speeds when a rotating disk electrode was used to maintain the steady-state mass-transfer conditions (not shown). On the other hand, the impedance plots shown in Figure 8 are completely overwhelmed by the Warburg impedance, which obscures the semicircles. Finally, both the Nyquist and amplitude vs log ω (Bode) plots approach rather ideal forms, which is hardly seen in the results obtained by conventional technique because of the difficulty in reaching an equilibrium situation for such a long measurement time (Figure 8). As a result, results obtained by our technique describes the system much better using the model shown in Figure 1 than those from the FRA method.

Since the comparison of the two different techniques is not possible for impedance results obtained in solutions due to heavy interference by the Warburg impedance (Figure 8) when the conventional FRA method is used, we prepared an electrical circuit with components of values similar to those shown in Figure 7. That is, the circuit shown in Figure 1 was constructed with $R_s = 4\ \Omega$, $R_p = 100\ \Omega$, and $C_d = 10\ \mu$F. Then, the measurements were made by both our FT and the FRA methods, and we obtained essentially the same impedance plots (not shown) as those shown in Figure 7. The individual values were in excellent agreement with each other within ±2%. These control experiments along with the results obtained from the rotating disk electrode convince us that the results shown in Figure 7 are real. We believe the discrepancies (of less than ±2%) shown between the two methods arose from the different relaxation properties of the electronic circuits used for two different measurement methods.

With the measurement system properly designed, more data points can be observed during the most important time span of about a few hundred microseconds. The faster the rise time of the potentiostat, the better the approximation of the ideal Dirac δ function would be and, thus, the better the impedance data obtained. Also, the bit resolution of the digitizer should be reasonably high at a shorter conversion time. In the present work, we used an 8-bit digital oscilloscope for a faster conversion time. While the 8-bit converter would be good enough for the demonstration of the concept, an analog-to-digital converter with a higher bit resolution and a very high conversion rate would be important parameters for acquiring high-quality impedance data. Also, repetitive signals were used in this preliminary work using the temporary circuit constructed on a breadboard, but a circuit allowing single-shot measurement is also needed. Work is in progress to implement these instrumental needs in our laboratory.

In conclusion, the technique we developed for impedance measurements is expected to revolutionize the electrochemical measurements. Because its measurement time is *very* short and the technique does not disturb the system much during the measurements, one may implement the technique by applying a small potential step at different bias potentials, while conventional electrochemical experiments such as cyclic voltammetry are being conducted. In this way, in situ impedance measurements can be made in real time while the cyclic voltammetric currents are recorded. This should be possible because of the very short time required for a complete measurement in the whole frequency region and also the small potential steps would not affect the dc currents. The short time taken for the measurements offers another important advantage over the conventional method. In conventional methods, the measurements are made after the system is fully equilibrated at a given bias potential. However, since it takes a long time to make impedance measurements for a frequency range between 50 kHz and submillihertz, the system itself changes as a result of electrolysis during the measurements or by the time the measurements are over. This problem is more severe than generally thought, and our technique solves this problem better than any other conceivable methods would have.

Another advantage our technique offers is that the measurements can be made between infinitely high frequencies and almost dc levels with a frequency resolution determined by the number of sampled points. As pointed out, the number of sampled points is made infinitely large by transforming from $t = -\infty$ to ∞ and the nth point included in the Fourier transform is resolved from the $n + 1$th and $n - 1$th points in any frequency range, although we took only 26 points/decade.

During the cyclic voltammetric scan, many different processes including adsorption of the reactants and/or products, as well as various following reactions, may take place, and thus, the state of the electrode may change at different potentials. These changes can be monitored in real time with our technique. Also, the technique can be implemented into battery testing during charging or discharging processes, where the state of the electrode may be monitored in situ in real time. For the reasons described thus far, our technique is expected to revolutionize the electrochemical measurements just as other in situ techniques, for example, spectroelectrochemical and quartz crystal microbalance experiments, have in identifying intermediate species during electrochemical experiments.

ACKNOWLEDGMENT

This research was supported by a grant from nondirected funds of Korea Science & Engineering Foundation (KOSEF 981-0305-028-2).

Received for review July 12, 1999. Accepted January 27, 2000.

AC9907540